Design, fabrication, assembly, and testing of the Florida Image Slicer for Infrared Cosmology and Astrophysics (FISICA) integral field unit

Paul Glenn[*a], Greg Hull-Allen[a], Jeff Hoffman[b], J. Michael Rodgers[b], Kevin Thompson[b], Bruce Myrick[c], Lovell Comstock[c], Scott Flint[c], Glenn Boreman[d], Stephen Eikenberry[e], Richard Elston[e], Rafael Guzman[e], Jeff Julian[e], Nicholas Raines[e]
[a]Bauer Associates, 888 Worcester Street, Suite 30, Wellesley, MA 02482
[b]Optical Research Associates, 3280 East Foothill Boulevard, Pasadena, CA 91107
[c]Corning Diamond Turning Division, 69 Island Street, Keene, NH 03431
[d]University of Central Florida, Center for Research in Electro-Optics, #400, PO Box 162700, Orlando, FL 32816-2700
[e]University of Florida, Department of Astronomy, 211 Bryant Space Science Center, Gainesville, FL 32611

ABSTRACT

We discuss the design, fabrication, assembly, and testing of the prototype Florida Image Slicer for Infrared Cosmology and Astrophysics (FISICA) Integral Field Unit (IFU). FISICA is intended for large telescopes with f/numbers close to f/15, such as the KPNO 4-m and GTC 10.4-m telescopes. It implements an image slicing approach, wherein the initial image plane is optically sliced into thin strips and the strips are optically rearranged end-to-end, whereupon the composite slit image is fed into a conventional spectrograph. We divide the field of view into 22 slices, while accommodating the entire f/15 viewing solid angle. The all-reflective instrument resides in a cryogenic dewar at the initial focal plane, and places the composite slit image output precisely at the initial focus, allowing it to interface to the existing FLAMINGOS spectrograph. The mirrors were diamond turned using various tool geometries and state-of-the-art, multi-axis tool control. The mirrors are made from a single billet of aluminum, and the optical bench and mounts are made of the same alloy as the mirrors for optimum performance during cryogenic cooling. We discuss the key design efforts, emphasizing tradeoffs among performance, volume, fabrication difficulty, and alignment requirements. We describe the fabrication, and present preliminary laboratory test results.

Keywords: image slicer, integral field spectroscopy, diamond turned mirrors, infra-red

1. INTRODUCTION

Imaging spectroscopy unavoidably poses the difficult task of separating spatial information from spectral information in an extended scene. Several hardware approaches, known as Integral Field Units (IFU's), are used, with varying tradeoffs between spatial field of view and resolution, spectral range and resolution, and throughput. A promising, relatively new approach is that of image slicing[1,2,3]. In this approach, the initial image plane is optically sliced into thin strips, and the strips are optically rearranged so that they lie end-to-end, at which point the entire composite slit image is fed into a conventional spectrograph. In this paper we describe the prototype Florida Image Slicer for Infrared Cosmology and Astrophysics (FISICA) IFU, which we have recently designed, built, and preliminarily tested in the laboratory. A companion paper to this one[4] reviews the image slicing approach to an IFU in general, discusses the prototype FISICA unit and its companion FLAMINGOS spectrograph in particular, and discusses current work and future plans regarding testing of the prototype FISICA in actual use.

[*] paul@bauerinc.com; phone 781-235-8775 x172; fax 781-235-2274; bauerinc.com

Ground-based Instrumentation for Astronomy, edited by
Alan F. M. Moorwood, Masanori Iye, Proceedings of SPIE Vol. 5492
(SPIE, Bellingham, WA, 2004) · 0277-786X/04/$15 · doi: 10.1117/12.551661

2. SYSTEM OVERVIEW AND CONFIGURATION

The basic imaging characteristics of FISICA are as follows:

- Telescope focal plane
  - Wavelengths: 1.0 – 2.5 microns
  - Focal plane size: 9.1 mm (along the slices) x 4.3 mm (across the slices)
  - Speed: f-15
  - Slicing: 22 slices, each 9.1 mm x 0.195 mm
  - Telecentric
- Output slit
  - Slit size: 100.0 mm (along the slit) x 0.098 mm (across the slit)
  - Speed: f-7.5
  - Telecentric
- System magnification (output size / input size)
  - [100 mm] / [22 * 9.1 mm] = 0.500
- Image inversion / rotation
  - None (i.e., non-inverting and non-rotating)

The tasks of FISICA are to break the telescope focal plane into 22 individual slices (or slitlets); rearrange the slices into a single slit; and place that slit optically at the same location as the telescope focal plane so that it can be viewed directly by a spectrograph. To accomplish these tasks, FISICA has the following major components:

- A three-mirror relay that magnifies the telescope focal plane to allow a larger image slicer
- The image slicer, which essentially consists of 22 slitlet mirrors, each one curved to relay the pupil image, and each one tilted in a different direction to redirect its slitlet appropriately
- A set of 22 powered imaging mirrors, placed approximately at an image of the telescope exit pupil
- A set of 22 powered field mirrors, placed at the image of the slicer mirrors as created by the imaging mirrors
- A pair of fold flats to redirect the ray bundles from the field mirrors so that the apparent source of the ray bundles is the telescope focal plane

Figure 1 shows a side view of the entire system. It shows the bundles of rays coming from the telescope focal plane at the top left. The rays then go through the following steps:

- They make three bounces off the mirrors of the relay, finally going to the left.
- They hit the slicer, finally going down and to the right.
- They hit the two rows of imaging mirrors, finally going up and to the left.
- They hit the field mirrors, which are situated *between* the two rows of beams going to the imaging mirrors. They finally go up and to the right.
- They hit the first fold flat, finally going up and to the left.
- They hit the second fold flat. At this point, Figure 1 shows the rays going to the left. However, these are *virtual* rays to show where the rays will *appear* to come from when seen by the spectrograph. The actual rays would go to the right, and would appear to emanate from the telescope focal plane (which is where the rays started in the first place).

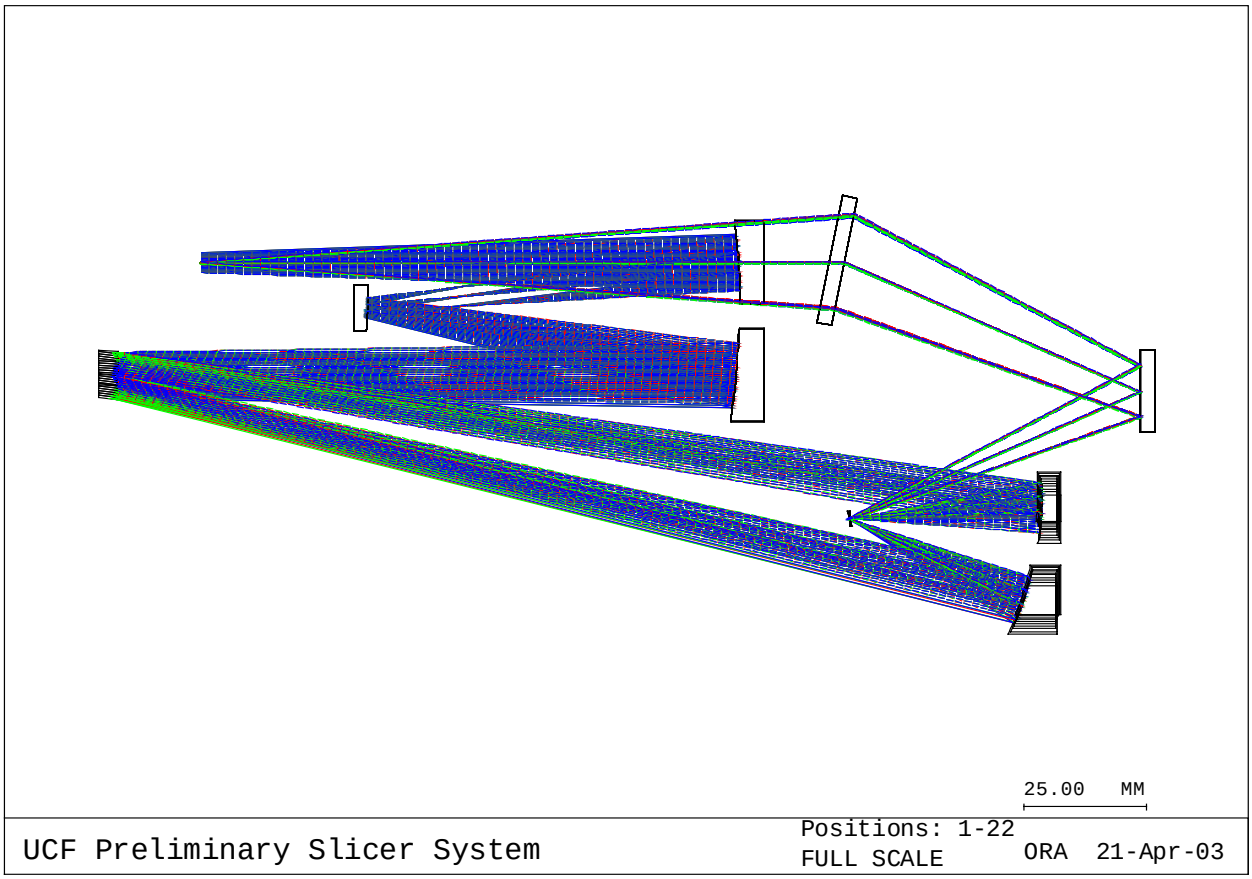

Figure 1. Side view of the prototype FISICA, including light rays.

Figures 2 and 3 show two views of the completed prototype FISICA. Figures 4 and 5 show the slicer mirror assembly and the imaging mirror assembly.

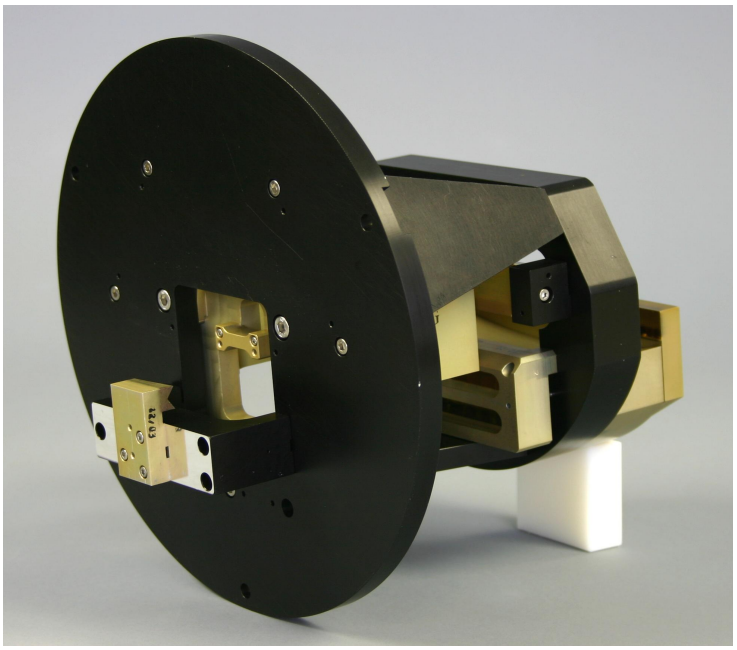

Figure 2. The prototype FISICA from the front and side. The slicer mirror assembly is the left-most mirror module, located on the front of the front aperture plate. The imaging mirror assembly is the right-most mirror module, located on the rear of the rear aperture plate.

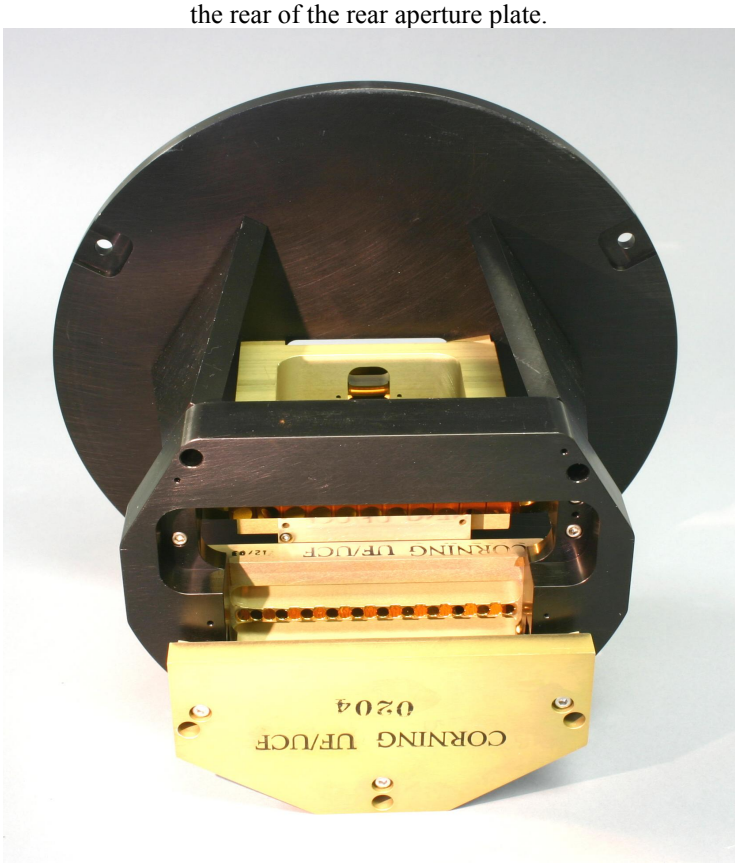

Figure 3. The prototype FISICA from the rear and top. The imaging mirror assembly is closest to the camera, although the imaging mirrors are not directly visible. The field mirrors are visible just above the imaging mirror assembly. And, at the top of the aperture in the rear aperture plate, some of the imaging mirrors are visible in the fold flat.

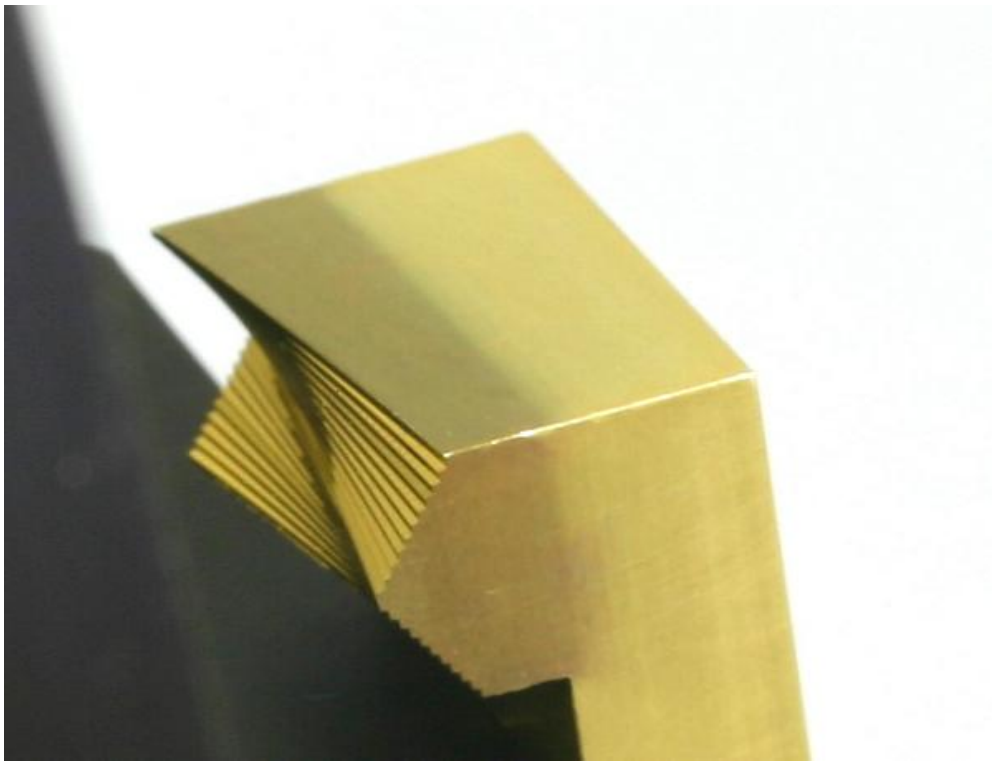

Figure 4. The monolithic slicer mirror assembly (gold-plated and overcoated aluminum). Note the clearly visible variation in azimuthal pointing angle, needed to steer the light from each slice to its appropriate imaging mirror. The curvature of the slices, needed to relay the pupil image onto the imaging mirrors, is also somewhat visible.

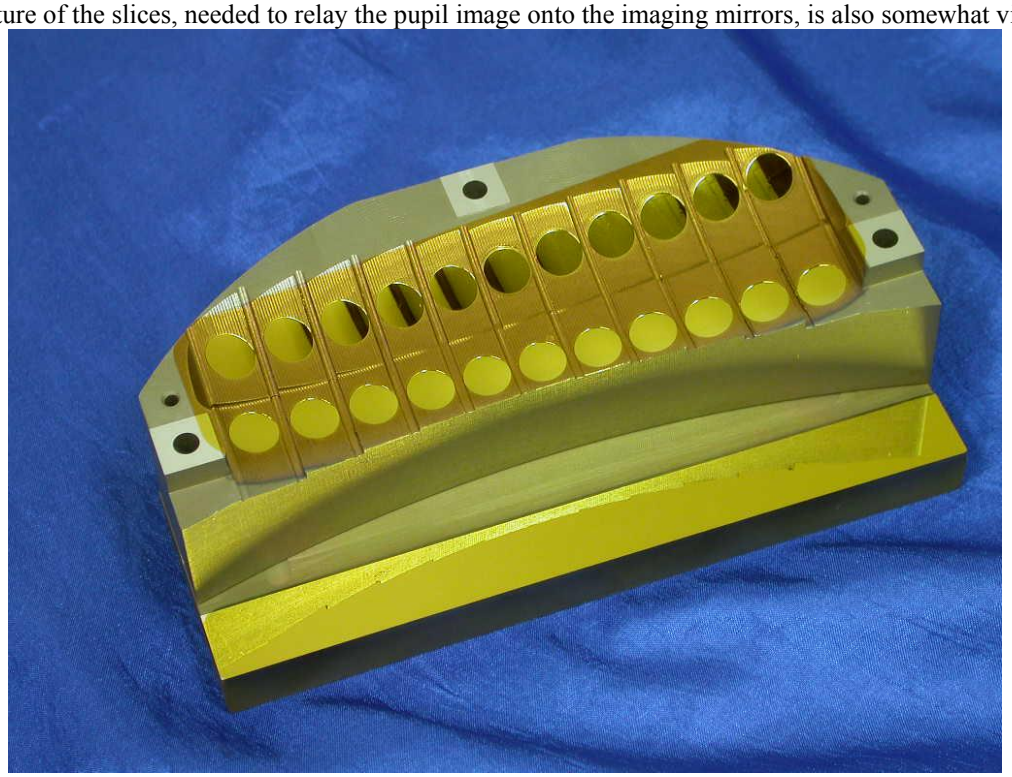

Figure 5. The monolithic imaging mirror assembly (gold-plated and overcoated aluminum). The 22 spherical mirror surfaces have different tilt angles and radii of curvature, but are diamond turned into a single monolithic substrate.

3. DESIGN TRADEOFFS

There were several tradeoffs to be made among performance, volume, fabrication difficulty, and alignment. The most basic question was whether to fabricate the mirrors for the 22 channels individually, or as monolithic modules containing all 22 channels of a particular mirror (slicer, imaging mirror, or field mirror). If the mirrors were made as monolithic modules, the fabrication could be complicated. But if the mirrors were made individually, the alignment could be nearly impossible, and unrecoverable in use if the system were somehow perturbed. We chose the monolithic approach for all three modules. (In fact, we made all of the optical components out of the same billet of aluminum, and made the structural components out of the same alloy as the mirrors in order to maintain the performance during cryogenic cooling.) Although the fabrication was complicated, we were able to build the system in such a way that it needed no alignment whatsoever. By using a combination of pins and precision-machined mounting surfaces, we were able to assemble and disassemble the system repeatedly with no impact on the alignment. With the exception of the need to remachine a single mounting surface to compensate for a fabrication imperfection (discussed further in Section 4), every aspect of the alignment was correct as fabricated.

Once the monolithic fabrication approach was selected, there were several tradeoffs and limitations to be considered. Some examples were as follows:

- In order to achieve accurate pointing angles on the slicer mirrors, and in consideration of the method in which the angles would be set during fabrication,
    - the azimuthal pointing angles needed to be separated by multiples of 30.00 arc-minutes; and
    - the elevational pointing angles needed to be identical on as many of the slices as possible (we used two banks of 11 slices, with each bank having its own constant elevational angle).
- The radius of curvature on the slicer mirrors needed to be the same for all 22 slices, and could not exceed a certain maximum value implied by the dimensions of the diamond turning machine.
- If we increased the magnification of the relay, the slicer would become larger and generally easier to fabricate. But, since the system magnification is fixed at 0.5, the larger demagnification required of the imaging mirrors would degrade the performance.
- If we increased the length of the optical paths to and from the imaging mirrors, the light would strike them at smaller incidence angles and performance would be improved. But, the volume of the package would increase to the point that it could no longer fit in the intended dewar.
- As indicated above, the angles of incidence on the imaging mirrors were key drivers of performance. Although the use of aspheric mirrors could improve the performance, we were reluctant to attempt their fabrication in the first prototype FISICA. Placing the field mirrors in between the two sets of beams going to the imaging mirrors (see Figure 1) turned out to be a very effective way of minimizing the incidence angles, but it complicated the mechanical layout.
- The field mirrors needed to reflect the beams away from the imaging mirrors and towards the two fold flats (again see Figure 1). This in turn required relatively high slope angles on the field mirrors, which made their fabrication more difficult (discussed further in Section 4).

As one might imagine, it was a considerable challenge to balance all of the tradeoffs and limitations above to come up with a design for a system that could be fabricated and that would perform well. As discussed in Section 4, though, we were successful.

4. PERFORMANCE GOALS AND PRELIMINARY TESTING RESULTS

The performance goals of the prototype FISICA were specified in terms of image quality and output telecentricity, as follows:

- Image quality:
    - 80% geometric encircled energy diameter at the slit plane to be less than 145 microns
- Telecentricity:
    - Chief rays of the 22 output bundles to be parallel to within approximately +/-5 milliradians

As implied by the term “geometric” encircled energy, the image quality goal was not to include the effects of pupil diffraction, nor the effects of surface scatter caused by roughness in the surface finish.

During the initial assembly, we performed several types of tests on both the image quality and the telecentricity. We also checked the location of the intermediate image to be sure it lay at the image slicer. And, we checked to be sure that the beams struck the various optical surfaces in the proper locations.

The test for proper beam locations on the various optical surfaces led to our finding one of the few minor problems in fabrication. Specifically, we found that the beams on the imaging mirrors were all displaced by the same amount elevationally (i.e., in the cross-slit direction). By examining Figure 1, one can see that various tilts or displacements of relay mirrors or the slicer assembly could cause this. After eliminating most of these possibilities, we determined through more detailed testing that the source of the error was a very slight but constant elevational error in every one of the 22 slicer mirrors. This error appears to have been caused by a residual imperfection in the diamond tool left by the break-in process prior to the actual turning of the slicer. Since the diamond tool is so small (a flat tip less than 0.5 mm wide), a small angular error in it is very hard to detect. Therefore, in future units, we may opt to make the elevational alignment of the slicer mirror assembly adjustable.

Apart from the minor slicer elevation angle problem, our initial tests showed that the mirrors were all fabricated with the proper radii of curvature and tilt angles, and that they were all placed in their correct locations and orientations by the structure. We were able to view an image of the slicer mirrors at the telescope focal plane with great clarity, confirming the basic operation of the three-mirror relay.

In the detailed image quality testing, we used two types of scenes. The first was a set of illuminated slits running across all 22 image slices. The intent was that each slitlet would show an identical picture. We arranged the illuminated slits so that only one half of the length of the slices would be illuminated, with the other half of the length being dark. Figure 6 shows several of the imaged slitlets.

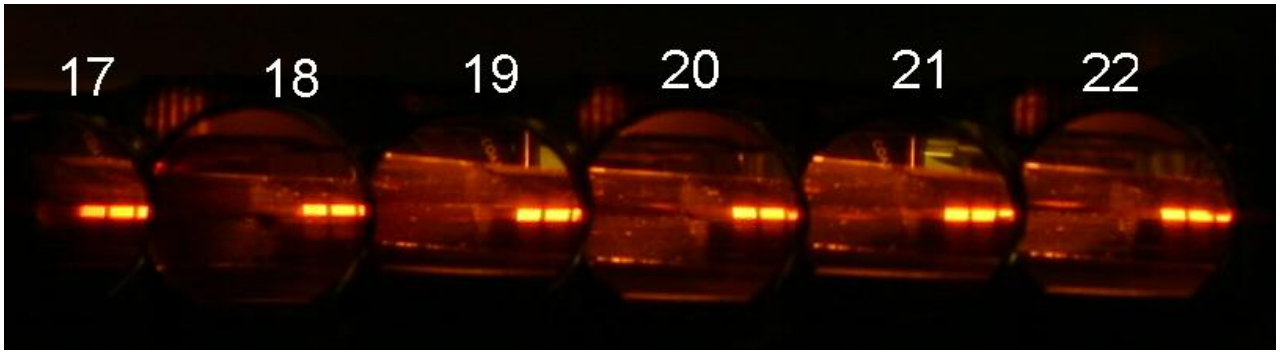

Figure 6. Several of the imaged slitlets with a scene consisting of a set of illuminated cross-slice slits. As expected, only approximately one half of each slitlet shows the illuminated slits, with the other half being dark.

(One interesting aspect of the image slicing that is not immediately apparent is that the slitlets (i.e., the individual slices) are interleaved in the spectrograph slit. In other words, if a point object were to traverse the telescope focal plane successively from slitlet to slitlet, it would make its appearance in *alternating* slitlets in the spectrograph slit plane, starting from one end and then returning to the other end in the remaining positions. Thus, the slitlets consecutively numbered 17-22 in Figure 6 are not consecutive in the telescope focal plane.)

The images in Figure 6 (and other photographs for the remaining slitlets) demonstrated that the imaging was fundamentally correct and reasonably sharp. However, examining the edges of the images failed to demonstrate the required image sharpness. We therefore used a pinhole as our second type of scene. We placed the pinhole, whose size was considerably smaller than the resolution goal (145 microns in the slit plane) within a single slice and photographed the image. Figure 7 shows the results, consisting of the photographic image on the left and the average radial intensity profile on the right.

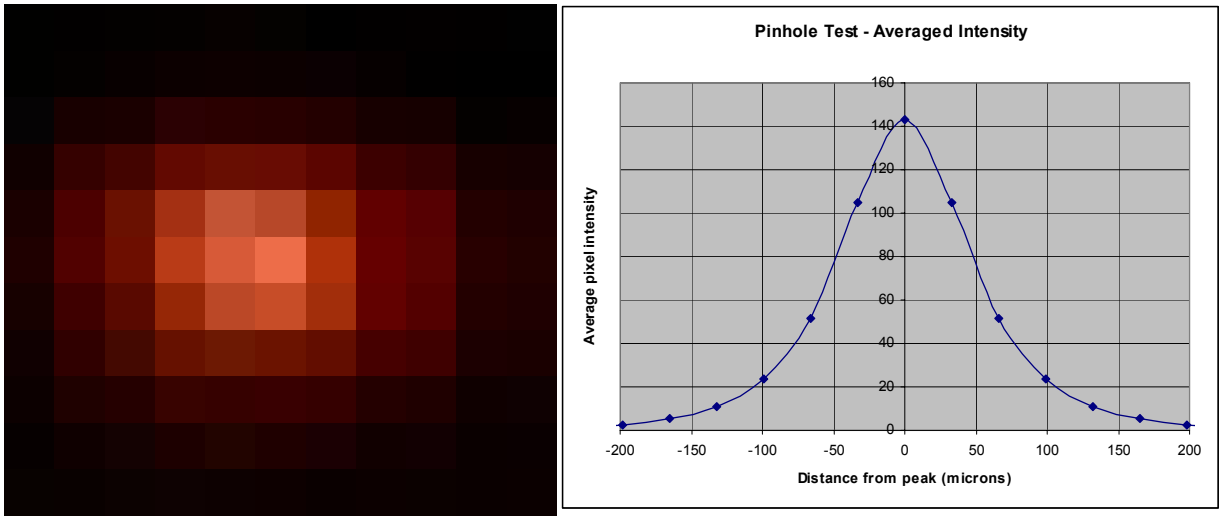

Figure 7. Pinhole test results. The photographic field on the left is approximately 360 microns wide. The plot on the right shows the average radial intensity.

We integrated the average radial intensity in Figure 7 to estimate the 80% encircled energy diameter, obtaining a value of 260 microns. This is considerably larger than the goal of 145 microns. However, the extended wings in Figure 7 suggest a non-negligible amount of larger-angle scatter due to roughness in the surface finish of the mirrors. We therefore reanalyzed the curve in Figure 7 in a way where we could concentrate on its core – in other words, its central region that was the motivation for the encircled energy specification. Specifically, we found the Full Width Half Maximum (FWHM) of the curve, and calculated the 80% encircled energy diameter *of a two-dimensional Gaussian image having that same FWHM.* In other words, by looking at the core of the image and postulating that it could be approximated by a Gaussian that characterized the true, scatter-free image core, we reassessed the 80% encircled energy diameter. Straightforward analysis of a two-dimensional Gaussian image yields the relationship

$$(80\%\_EE\_diameter) = (FWHM)\sqrt{\frac{\ln(5)}{\ln(2)}} \approx (1.524)(FWHM) \tag{1}$$

In order to push this analysis even further into the core of the image, we also used a corresponding relationship involving the full-width-70%-maximum diameter:

$$(80\%\_EE\_diameter) = (FW\_70\_M)\sqrt{\frac{\ln(5)}{\ln\left(1/0.70\right)}} \approx (2.124)(FW\_70\_M) \tag{2}$$

The results of these analyses are listed in Table 1.

Estimation method	**Estimated 80% encircled energy diameter**
Integration of fitted radial intensity curve	260 microns
Equate to a 2-d Gaussian image with the same Full Width Half Maximum (FWHM)	151 microns
Equate to a 2-d Gaussian image with the same Full Width 70% Maximum (FW_70_M)	141 microns

Table 1. Assessment of the 80% encircled energy diameter, first by direct integration of Figure 7, and then by detailed assessment of the image core.

Table 1 indicates that the image quality generally meets the goal of a geometric 80% encircled energy diameter of 145 microns. However, it also indicates that the larger-angle scatter is non-negligible, at least at our visible testing wavelengths. We expect the scattering to improve at the in-use wavelength range of 1.0-2.5 microns, but will need to wait for actual images to assess the improvement.

To test the telecentricity, we illuminated the telescope focal plane with a slit of collimated light, with the slit again running across the slices. We then simply measured the lateral displacements of the slitlet images after they had propagated by a large, known distance from the slit plane. The results are shown graphically in Figure 8, which has separate plots for the slit scene being located at each end of the slices in turn. (The points in the plots are connected in order of their appearance in the slit plane, *not* in order of their location in the telescope focal plane.)

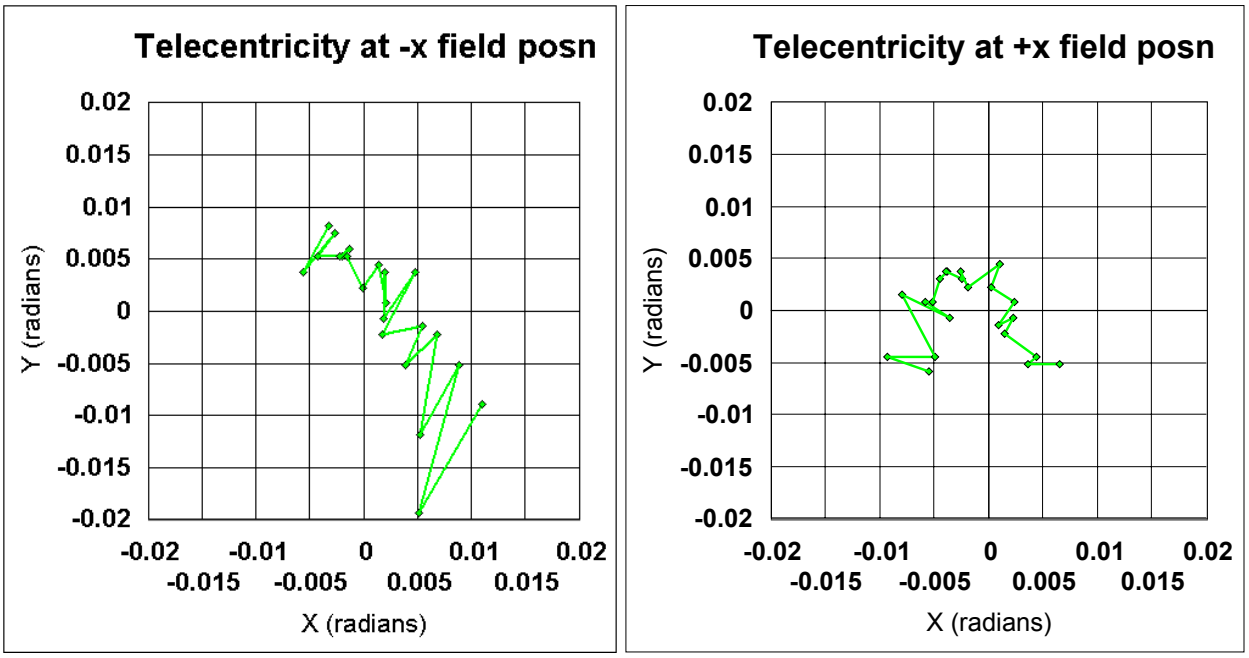

Figure 8. Telecentricity measurement results for images from each end of the slices in turn.

The RMS values considering all 22 slices and both field angles are as follows:

- RMS x-telecentricity error: 3.9 mrad
- RMS y-telecentricity error: 5.8 mrad
- RMS total telecentricity error: 7.0 mrad

These numbers are approximately a factor of two higher than the predictions for a perfect system. However, they compare reasonably well with the goal of approximately +/- 5 milliradians. The preliminary conclusion here, then, is that the telecentricity goals, while not literally met, were nearly met.

Notwithstanding the generally good results described above, there was a separate telecentricity problem that was more difficult to characterize. This was caused by localized slope errors on the field mirrors, which appeared under very careful examination as dimples on the centers of the mirrors. The magnitude of the dimples correlates very strongly with the magnitude of the slopes of the mirrors. This led us to conclude that they were due to tiny residual errors in the alignment of the diamond tool. These effects have been observed previously in the particular, state-of-the-art technique used to turn these tilted mirrors. And, these effects do indeed increase with the slope of the mirror being turned. In future efforts we may be able to reduce the effect by compensating in software for an inferred misalignment. We can also reduce the effect by turning the mirrors off-center, so that any residual defects are outside the slit apertures of the field mirrors. The effect can actually be reduced on the prototype FISICA by displacing the field mirror array.

The dimples manifest themselves by deflecting the light away from its intended path. In other words, in the telecentric view of the spectrograph, there will be losses in intensity at the centers of the slitlets afflicted by the dimples. Figure 9 shows a typical slitlet image unaffected by a dimple, and the worst-afflicted slitlet for comparison. (Most of the slitlets have no dimples.) The stripes above the vertically centered slitlets are unimportant ghost images arising from illuminating the system with light outside its nominal working f-number.

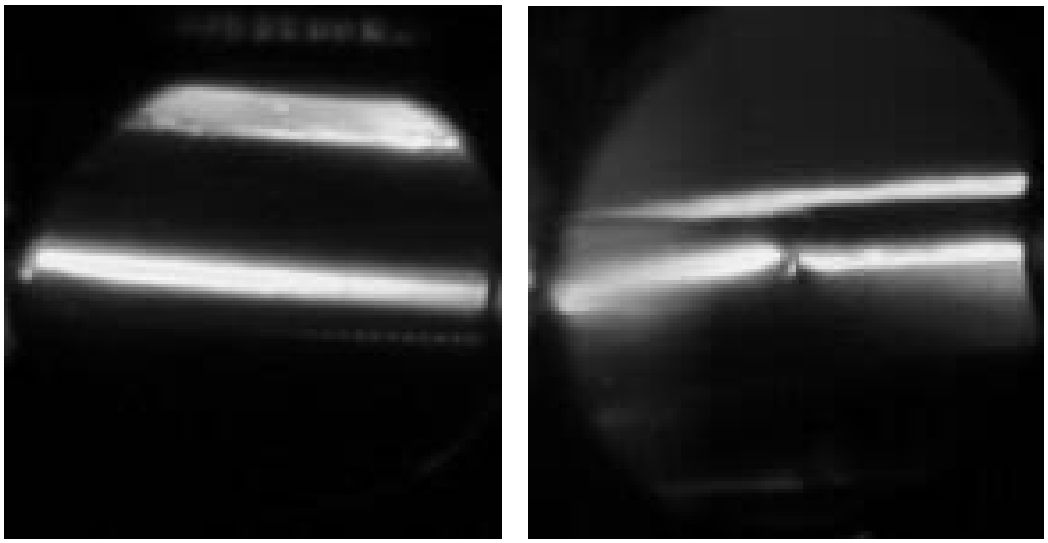

Figure 9. A typical slitlet image is on the left, and the slitlet with the worst dimple is on the right. (Most slitlets have no dimples.) The stripes above the vertically centered slitlets are unimportant ghost images arising from illuminating the system with light outside its nominal working f-number.

At the time of publication of this paper, the prototype FISICA is about to undergo its first actual telescope tests. It has gone through room-temperature and cryogenic tests at the telescope site, with the results being consistent with those described above.

5. SUMMARY

We have designed, built, and preliminarily tested the prototype Florida Image Slicer for Infrared Cosmology and Astrophysics (FISICA) Integral Field Unit (IFU). This image slicer system breaks the telescope focal plane into 22 individual slices (or slitlets); rearranges the slices into a single slit; and place that slit optically at the same location as the telescope focal plane so that it can be viewed directly by a spectrograph. Preliminary testing has demonstrated high-quality imaging and good telecentricity performance as we head into the first actual telescope tests. We have identified several small technological improvements that will help us get even better performance out of future units.

REFERENCES

1. R. Content, *A new design for integral field spectroscopy with 8-m telescopes*, Proc. SPIE 2871, pp. 1295-1305, 1997
2. R. Content, *Advanced image slicers for integral field spectroscopy with UKIRT and Gemini*, Proc. SPIE 3354, pp. 187-200, 1998
3. C.M. Dubbeldam *et al*, *An integral field unit for the Gemini near-infrared spectrograph*, Proc. SPIE 4008, pp. 1181-1192, 2000
4. S. Eikenberry *et al*, *FISICA: a monolithic image slicing integral field unit for FLAMINGOS*, Proc. SPIE 5492, 2004